Available online at www.sciencedirect.com
ScienceDirect
Journal of Hazardous Materials 157 (2008) 25–33
Journal of Hazardous Materials
www.elsevier.com/locate/jhazmat

Effect of bromide ion on isolated fractions of dissolved organic matter in secondary effluent during chlorination

Shuang Xue [a,c], Qing-Liang Zhao [a,b,*], Liang-Liang Wei [a], Ting Jia [a]

[a] School of Municipal & Environmental Engineering, Harbin Institute of Technology, Harbin 150090, China
[b] State Key Laboratory of Urban Water Resources and Environment (SKLUWRE), Harbin Institute of Technology, Harbin 150090, China
[c] School of Environmental Science, Liaoning University, Shengyang 110036, China

Received 21 September 2007; received in revised form 19 December 2007; accepted 19 December 2007
Available online 26 December 2007

Abstract

The role of bromide ion in the trihalomethane (THM) formation and structure of dissolved organic matter (DOM) during chlorination of the secondary effluent taken from the Wenchang Wastewater Treatment Plant (Harbin, China) was investigated. DOM was fractionated using XAD resins into five fractions: hydrophobic acid (HPO-A), hydrophobic neutral (HPO-N), transphilic acid (TPI-A), transphilic neutral (TPI-N) and hydrophilic fraction (HPI). The patterns of individual THM species with increased bromide concentrations were similar for all DOM fractions. The THM speciation as well as halogen fraction for these five fractions followed similar trends with the Br^-/Cl_2 ratio. Chlorination resulted in decreased ultraviolet (UV) absorbance across wavelengths from 250 to 280 nm for DOM fractions whether bromide ions existed or not, and bromide addition led to lower differential UV absorbance values. Fourier-transform infrared (FT-IR) results indicated that chlorination, whether bromide ions existed or not, resulted in the near elimination of aromatic C─H and amide peaks, increased C─O absorption intensity and occurrence of C═O and C─Cl peaks for HPO-A, HPO-N, TPI-A and TPI-N. Furthermore, bromide addition in chlorination led to the occurrence of C─Br peak for all four fractions.

Keywords: Dissolved organic carbon; Trihalomethanes; Bromide ion; Chlorination; FT-IR

1. Introduction

Chlorination is by far the predominant disinfection method for disinfecting secondary effluents [1]. It is generally known that dissolved organic matter (DOM) could potentially be converted to harmful disinfection by-products (DBPs) during chlorination, such as trihalomethanes (THMs) and haloacetic acids (HAAs). THMs are identified as potential adverse health agents and usually measured in terms of the sum of four methane derivatives, i.e., chloroform ($CHCl_3$), bromodichloromethane ($CHCl_2Br$), dibromochloromethane ($CHClBr_2$) and bromoform ($CHBr_3$) concentrations [2].

To better understand the formation of THMs, one can characterize DOM. The differentiation between each DOM species might not be practical and therefore several past researches focused on grouping DOM into several common groups according to the physical/chemical properties of DOM, e.g., polarity, size, molecular weight, etc. [2,3]. XAD resin method has been reported in many applications for fractionation of DOM and is generally considered as the state-of-art method at present for such fractionation [4]. The fractionation allowed a thorough investigation of the THM formation and spectral characterization of the DOM fractions [2,4]. Spectroscopic techniques such as ultraviolet–visible (UV–vis) and Fourier-transform infrared (FT-IR) have been previously applied for characterization of DOM [5–8]. The method employing an FT-IR analyzer to measure the spectrum of natural organic matter (NOM) has been accepted as an adequate way to estimate the humic properties [4].

* Corresponding author at: School of Municipal & Environmental Engineering, Harbin Institute of Technology, Harbin 150090, China.
Tel.: +86 45186283017; fax: +86 45186282100.
E-mail address: qlzhao@hit.edu.cn (Q.-L. Zhao).

0304-3894/$ – see front matter © 2007 Elsevier B.V. All rights reserved.
doi:10.1016/j.jhazmat.2007.12.071

In water supplies, the important factors affecting the formation of DBPs upon chlorination include the concentration and property of organic precursors, disinfectant type and dosage, pH, temperature, bromine ion content, etc. [9,10]. In the presence of bromide, free chlorine (hypochlorous acid, HOCl) rapidly oxidizes bromide to form hypobromous acid (HOBr), which then reacts with precursor materials to produce brominated organic DBPs. Since some brominated organic DBPs (such as bromine-containing THMs) pose more significant health risks than chlorinated analogs [1,11], ongoing research into the role of bromide in the formation and speciation of DBPs during chlorination of natural waters is of particular interest.

Yet, the THM formation during chlorination of wastewater and reclaimed water has so far received much less attention [1]. Wistrom et al. [12] developed a simple method to experimentally determine the air toxics emission potential of THMs as a result of wastewater chlorination using a flexible bag, zero-head-space reactor, and estimated the rate of THM production and the potential THM concentration for three wastewaters chlorinated at two chlorine doses. Koukouraki and Diamadopoulos [13] proposed exponential models for the THM formation during chlorination of nitrified and partially nitrified secondary effluents, as well as tertiary effluent. Yang et al. [1] studied the formation of THMs and HAAs from the breakpoint chlorination of three wastewater effluents and found that the concentrations and distributions of THM and HAA species varied among different effluents at different zones of the breakpoint curves. Matamoros et al. [14] investigated the THM concentrations in three chlorinated effluents (i.e., secondary and tertiary) from full-scale wastewater treatment plants in NE Spain over a 2-year monitoring period and reported that the THM formation showed a negative correlation with initial ammonia nitrogen concentration and total organic carbon concentration. However, the impact of bromide ion on the formation and speciation of THMs during chlorination of DOM fractions in secondary effluents still remains unclear. Moreover, the structural characteristics of DOM fractions in secondary effluents and the effect of bromide ion on the structural and chemical characteristics of the DOM fractions during chlorination have been rarely studied. Secondary effluents, which contain large amounts of organic matter, are likely to be major contributors to the genesis of DOM in major rivers [15]. Further investigation of the THM formation during chlorination of secondary effluents is needed, because many secondary effluents might be eventually discharged to water bodies that could later be utilized as sources of drinking water supply after undergoing a series of treatment.

The objectives of this study were to investigate the effect of bromide ions on the formation and speciation of THMs and structural characteristics of DOM fractions during chlorination of secondary effluent taken from the Wenchang Wastewater Treatment Plant (WWTP) (Harbin, China). Such knowledge can assist in our understanding of the interactions of chlorine with DOM in secondary effluents, and thus provides improved insight into the development of more effective control of THM formation before reuse or discharge of secondary effluents.

2. Materials and methods

2.1. Chemicals

All chemical solutions were prepared from reagent-grade chemicals or stock solutions. Milli-Q water (ELGA, Ultra Analytical) was used for all dilutions, sample and chemical preparation, and final glassware cleaning in this work. Solutions were stored at 4 °C and brought to room temperature before use. A chlorine solution was prepared in the form of concentrated sodium hypochlorite (3000 mg/L) and it was periodically standardized by DPD ferrous titrimetric method according to standard method 4500-Cl F [16].

2.2. Sample collection and preservation

Five hundred litres of non-disinfected secondary effluent was collected on 5 March 2007 from the WWTP, which was used for all experiments in this work. Samples were prepared by filtering through a 0.45 μm membrane and stored in a cold room with a temperature controlled at 4 °C before and after fractionation. Each filter was rinsed with 1000 mL Milli-Q water to remove any residual organic contaminants before use [17]. Water quality characteristics of the secondary effluent were: dissolved organic carbon (DOC) = 16.4 mg/L, ultraviolet absorbance at 254 nm (UV-254) = 0.216 cm^{-1}, NH_4^+ = 2.7 mg N/L, TKN = 5.0 mg N/L and Br^- < 20 μg/L (the detection limit).

2.3. Fractionation and isolation

DOM was fractionated into five classes: hydrophobic acid (HPO-A), hydrophobic neutral (HPO-N), transphilic acid (TPI-A), transphilic neutral (TPI-N) and hydrophilic fraction (HPI), using XAD-8/XAD-4 resin chromatography following established methods [18,19]. Briefly, 0.45 μm filtrates were acidified to pH 2 and passed through two columns in series containing XAD-8 and XAD-4 resins. HPO-A and TPI-A were eluted from the XAD-8 and XAD-4 columns, respectively, using 0.1 mol/L NaOH. HPO-N and TPI-N were those compounds that adsorbed onto XAD-8 and XAD-4 resins, respectively, but were not dissolved during back elution with NaOH. HPI was the carbon not retained on either resin. A complete description of isolation methods is given in [20]. The total weight of all DOM fractions was about 7% more than the original weight in the water sample. This might be due to the resin bleeding during elution processes, which was reported to result in a weight surplus in the resulting organic fractions [3]. Although the tolerance of DOM recovery for the fractionation method, which was employed in this study to fractionate DOM into five fractions, was not previously reported, this level of inaccuracy was considered acceptable as the tolerance of 10–15% was reported for another fractionation method fractionating DOM into six fractions [2].

2.4. Effect of bromide ion on the THM formation from DOM fractions

All samples were diluted with Milli-Q water to produce a DOC concentration of 1 mg/L before chlorination. Because each of the samples had the same DOC concentration, differences in reactivity with chlorine could be attributed to differences in the structural character of the samples.

Chlorination was performed on samples buffered with 0.05 mol/L phosphate at pH 7.0 ± 0.1. There were five waters solely containing HPO-A, HPO-N, TPI-A, TPI-N and HPI, respectively. For each water, 10 bromide concentrations, 0–16.7 μmol/L (Br^-/DOC ratio: 0–200 μmol/mmol), were added to form a five by ten matrix. Chlorine was added as sodium hypochlorite at a dose of 5 mg Cl_2/mg C. The chosen chlorine dose provided a free chlorine residue of at least 0.3 mg/L in all samples after 7 d. Chlorinated samples were incubated at 20 °C in the dark for 24 h in headspace-free 250-mL, glass-stoppered BOD bottles. After 24 h, the samples were quenched with ammonium chloride, and the THM concentrations were analyzed.

2.5. Effect of bromide ion on the structure of DOM fractions during chlorination

Experiments were conducted on HPO-A, HPO-N, TPI-A and TPI-N solutions. There were two sub-samples of each solution. One was added with bromide to achieve a Br^-/DOC ratio of 200 μmol/mmol and the other was without bromide addition. All samples were chlorinated with a chlorine dosage level based on 5 times the DOC concentration. After reacting for 7 d at 20 °C in the dark, the samples were dechlorinated with ammonium chloride, re-acidified to pH 2, and separately reapplied onto the respective columns. Retained organics were desorbed from the XAD resins using a 75% acetonitrile/25% Milli-Q-water solution. Acetonitrile was subsequently removed using rotary-evaporation and the resin isolates were lyophilized. The carbon in the XAD resin effluents were desalted using cation and anion exchange resins and lyophilized. The two separate lyophilized isolates from the same sample were collected together. The overall rate of recovery of the chlorinated DOCs varied between 76% and 89%. Isolates of the DOM fractions both before and after chlorination were analyzed using the FT-IR spectrometer, and dissolved in Milli-Q water prior to UV–vis spectrophotometric analysis.

2.6. Analytical methods

DOC was analyzed in triplicate on a Shimadzu TOC-5000 Total Organic Carbon Analyzer. The relative standard deviation (RSD) was <2% for DOC >2 mg/L, and <5% for DOC <2 mg/L. Bromide ion concentrations were determined using a Dionex ion chromatographic (IC) system (Sunnyvale, CA). THMs were extracted with methyl-tert-butyl ether (MTBE) from the chlorinated samples using a modified EPA method 551.1 and analyzed by gas chromatography with an ECD (Hewlett Packard 5890 II). THM measurements for all samples were performed in duplicate. For samples with relative-percent differences of the duplicates that exceeded 5%, the experiments were performed again. A multi-wavelength UV/VIS spectrophotometer (Shimadzu UV-2550) with a 1-cm cell pathlength was used to measure the UV absorbance of DOC at wavelength ranging from 250 to 280 nm. An estimate of the precision of the UV absorbance analysis was obtained by measuring two separate UV spectra from the same sample. The UV absorbance in the range of 250–280 nm was found to have a RSD from 0.3% to 3.7% for these samples. Infrared spectra were obtained using 2–5 mg of DOM fraction isolates in potassium bromide pellets. The PerkinElmer Spectrum One B FT-IR spectrometer was set to scan from 4000 to 400 cm^{-1}. All spectra were baseline corrected and normalized after acquisition to a maximum absorbance of 1.0 for comparative purposes [21–23]. Duplicate spectra for each sample demonstrated that the wavelength of IR absorption peaks was reproduced within ±3 nm; absorption intensities replicated within ±5.1%.

3. Results and discussion

3.1. Effect of bromide on THM formation

The formation of THM in the five fractions, i.e., HPO-A, HPO-N, TPI-A, TPI-N and HPI, spiked with bromide is shown in Fig. 1. In general, total THM concentrations for HPO-N, TPI-A, TPI-N and HPI were fairly constant over the range of bromide concentrations studied. For HPO-A, however, an increase in total THM concentration with increasing bromide concentration was noted in the region of bromide concentration (1.67–7.5 μmol/L). As shown in Fig. 1a, HPO-A consistently exhibited the highest total THM concentration and TPI-A showed the second total THM concentration within the range of bromide addition used. Total micromolar THM formation from HPO-N, TPI-N and HPI were close and overlapped at several points. The results indicated that HPO-A was the most active fraction in forming THMs while TPI-A was the second. The reactivity of HPO-N, TPI-N and HPI were not significantly different ($p > 0.05$), which were significantly lower than that of HPO-A and TPI-A ($p < 0.05$).

The patterns of individual THM species with increased bromide concentrations were similar for all DOM fractions, which were as follows: $CHCl_3$ decreased exponentially; $CHCl_2Br$ and $CHBr_2Cl$ increased initially and then decreased, with the peaks occurring at bromide concentrations of 0.8–3.3 μmol/L and 7.5–10.0 μmol/L, respectively; $CHBr_3$ increased continuously (Fig. 1b–e). Increasing bromide concentration gradually shifted THM speciation from chlorinated species to mixed bromochloro species to brominated species during chlorination of DOM fractions.

3.2. Effect of bromide on THM speciation

The molar ratio of bromide to applied chlorine is an important factor for THM formation and speciation. The relative concentrations of the four THMs from each fraction, expressed as molar percentages of the total THM concentration, were plot-

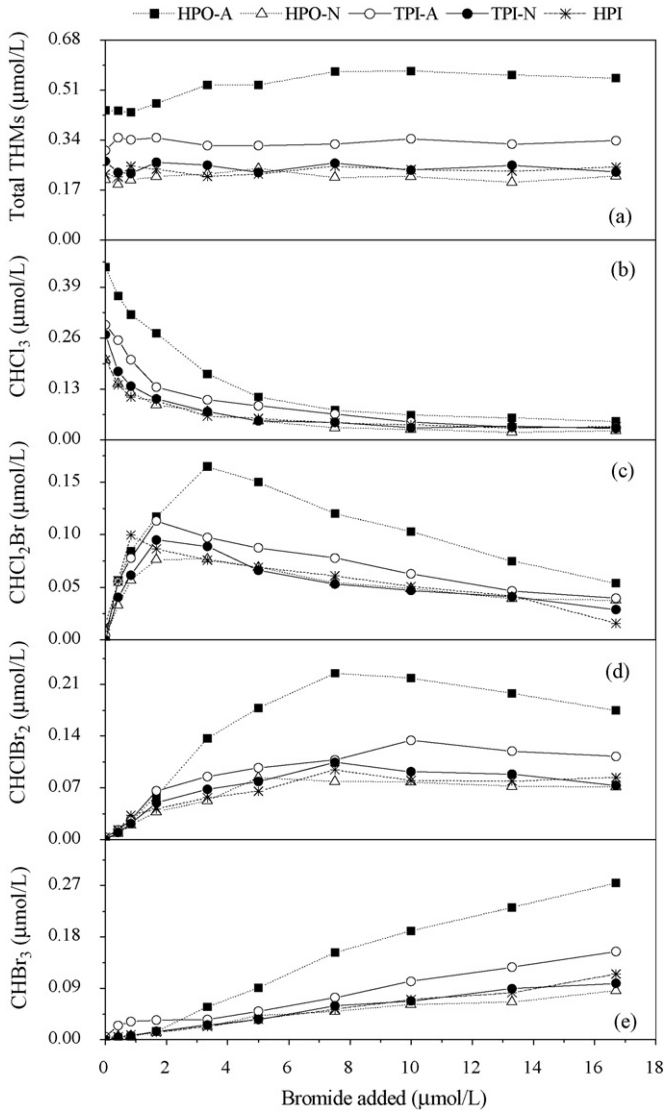

Fig. 1. Effect of bromide concentration on the formation of (a) total THMs, (b) $CHCl_3$, (c) $CHCl_2Br$, (d) $CHClBr_2$ and (e) $CHBr_3$ from DOM fractions.

ted as a function of Br^-/Cl_2 ratio in Fig. 2. Generally speaking, THM speciation in these five fractions followed similar trends with Br^-/Cl_2. Under the experimental conditions investigated, $CHCl_3$ monotonically decreased and $CHBr_3$ monotonically increased with increasing Br^-/Cl_2. However, $CHCl_2Br$ and $CHBr_2Cl$ peaked within the range of Br^-/Cl_2 ratios encountered. Even at the lowest Br^-/Cl_2 ratio (0.05 μmol/mmol), the bromine-containing THMs ($CHCl_2Br + CHBr_2Cl + CHBr_3$) from each DOM fraction constituted at least 16% of the corresponding total THMs on a molar basis. Mole fraction of these bromine-containing THMs increased rapidly with Br^-/Cl_2 before reaching an asymptotic value of ~90%.

In addition to Br^-/Cl_2, changes in Br^-/DOC also influence THM formation and speciation [19]. In this study, the Cl_2/DOC ratio was fixed at 0.85 mmol/mmol, while Br^-/DOC and Br^-/Cl_2 were varied simultaneously in the range 0–200 and 0–240 μmol/mmol, respectively. Thus, the Br^-/DOC ratio increased with increasing Br^-/Cl_2. THM speciation shifted

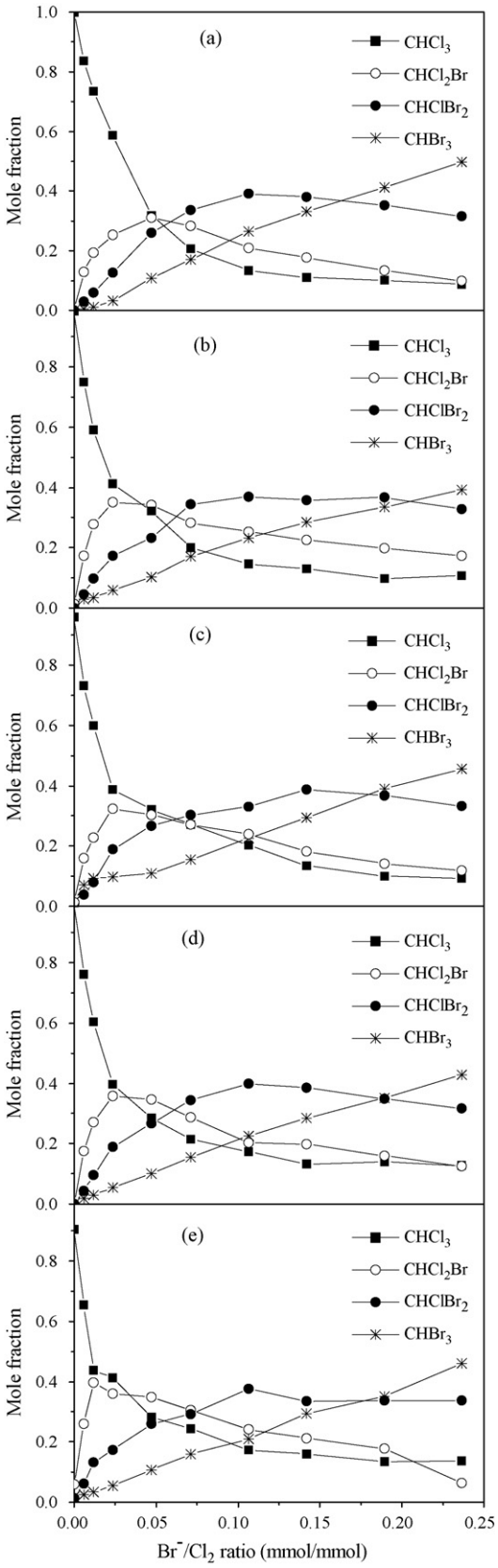

Fig. 2. Mole fractions of individual THM species for (a) HPO-A, (b) HPO-N, (c) TPI-A, (d) TPI-N and (e) HPI as a function of Br^-/Cl_2 molar ratio.

toward the more brominated species in the five fractions due to increases in both Br^-/Cl_2 and Br^-/DOC.

Chang et al. [24], Uyak and Toroz [25] also studied THM speciation in natural waters by fixing the Cl_2/DOC ratio but varying Br^-/DOC and Br^-/Cl_2 simultaneously. In the study conducted by Chang et al. [24], $CHBr_3$ was about 50% of total THMs at $Cl_2/Br^- = 7$, and the sum of $CHCl_2Br$ and $CHBr_2Cl$ was 79% of total THMs at $Cl_2/Br^- = 9$. Similar results were also reported by Uyak and Toroz [25], or 75% and 97% for $Cl_2/Br^- = 3.4$ and 5.6, respectively. The relative concentrations of bromine-containing THMs in this study were significantly low in comparison with those previously reported, as demonstrated by the molar fractions of 39–50% and 28–33% for $CHBr_3$ from the five fractions at $Cl_2/Br^- = 4.2$ and 7, respectively, and also the molar fractions of 49–56% and 57–62% for the sum of $CHCl_2Br$ and $CHBr_2Cl$ at $Cl_2/Br^- = 5.3$ and 9.4, respectively. The results suggested that bromine-containing THMs were favored over $CHCl_3$, to a lesser extent, for the five fractions isolated from the secondary effluent than for NOM in natural waters. Although the Br^-/DOC ratio is also an important factor to be considered while examining THM formation and speciation, it was impossible to determine whether the differences in Br^-/DOC between various studies resulted in the distinct relative concentrations of bromine-containing THMs at similar Cl_2/Br^- ratios, as the Br^-/DOC ratios corresponding to the relative concentration values reported were not presented simultaneously in the literatures.

Chellam and Krasner [26] investigated the formation and speciation of DBPs resulting from chlorination of nanofilter permeates obtained from various source water locations and membrane types, and reported that $CHCl_2Br$ that contains 1 mol Br/mol THM peaked at 12 μmol/mmol Br^-/DOC compared to $CHClBr_2$ that contains 2 mol Br/mol THM and peaked at approximately twice the Br^-/DOC at 25 μmol/mmol. In the present study, $CHCl_2Br$ from HPO-A, HPO-N, TPI-A, TPI-N and HPI peaked at 3.33, 3.33, 1.67, 1.67 and 0.83 μmol/mmol Br^-/DOC, respectively, whereas $CHClBr_2$ from all the DOM fractions peaked at the same Br^-/DOC (7.5 μmol/mmol), with the exception of that from TPI-A which peaked at 10 μmol/mmol Br^-/DOC. Only for HPO-A and HPO-N, $CHClBr_2$ peaked at about twice the Br^-/DOC ratio at which $CHCl_2Br$ peaked.

3.3. Effect of bromide on halogen fraction

Bromine fraction has been used as an unbiased measure of bromine substitution among different DBP classes [27]. It was defined as the ratio of the molar concentration of bromine incorporated into a given class of DBP to the total molar concentration of chlorine and bromine in that class [28]. Similarly, molar percent chlorine is termed chlorine fraction.

As can be expected, increases in Br^-/Cl_2 increased bromine fraction, while decreasing chlorine fraction (Fig. 3). Bromine and chlorine fraction were equivalent in the range of Br^-/Cl_2 molar ratio (0.07–0.10) for all DOM fractions, suggesting that HOBr is more reactive than HOCl in substitution and addition reactions that form THMs (Fig. 3).

Because halogen fractions for all these fractions followed strikingly similar trends with the Br^-/Cl_2 ratio, it suggested that the Br^-/Cl_2 molar ratio was a more important factor in determining both bromine and chlorine fractions than was the DOM type. Thus, the Br^-/Cl_2 molar ratio can be a useful tool to predict or model halogen substitution during chlorination.

3.4. Effect of bromide on DOM structure

3.4.1. UV spectroscopic analysis

The UV absorbance of organic matter, in the range of 250–280 nm, reflects the presence of sp^2-hybridized carbon (e.g., aromatic carbon) [29,30]. It was reported that chlorine attacks NOM predominantly at activated aromatic sites or conjugated double bonds, which absorb UV light effectively at wavelengths of 250–280 nm, and chlorination changes this region of UV absorbance spectra of NOM as a result of alteration and destruction of these sites [31,32]. Fig. 4a shows the UV spectra for DOM fractions prior to chlorination. Although the spectra appeared to be broad and featureless, the absorption intensity varied greatly among the four DOM fractions; their relative order of intensity was HPO-A > HPO-N > TPI-A > TPI-N in the range of 250–278 nm, suggesting that HPO-A contained a relatively high amount of aromatic or polyphenolic organic compounds as compared to the other fractions.

The differential UV spectrum for each DOM fraction (DOC = 1 mg/L) reaction with chlorine in the absence of bromide is shown in Fig. 4b, which was calculated by subtracting the absorbance of post-chlorination sample without bromide addition from that of the corresponding pre-chlorination sam-

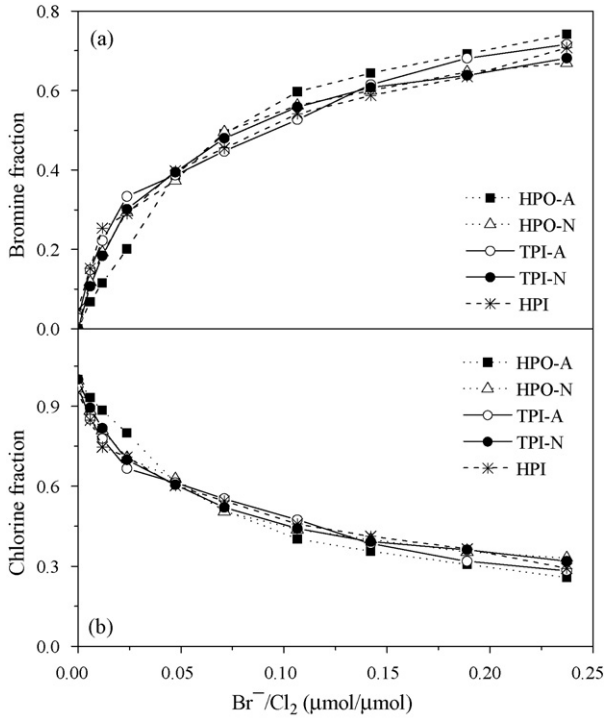

Fig. 3. Effect of Br^-/Cl_2 molar ratio on (a) bromine fraction and (b) chlorine fraction for DOM fractions.

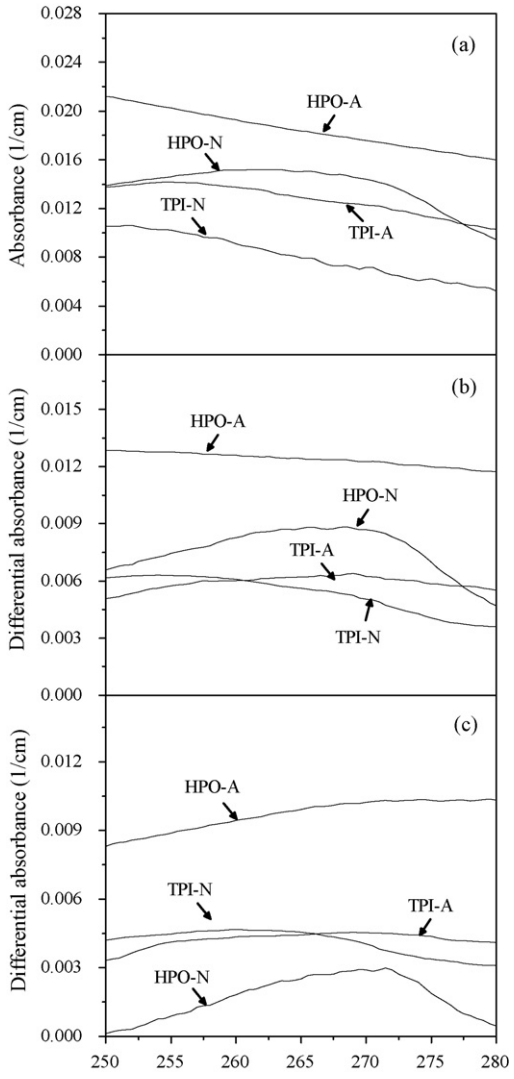

Fig. 4. UV spectra for pre-chlorination DOM fractions (a), and differential UV spectra for post-chlorination DOM fractions without bromide addition (b) and for post-chlorination DOM fractions with bromide addition to achieve a Br^-/DOC ratio of 200 μmol/mmol (c). All spectra were obtained in samples adjusted to 1 mg/L of DOC.

ple. Similarly, Fig. 4c shows the differential UV spectra of the bromide-added samples during chlorination. A positive value for the differential spectra across wavelengths from 250 to 280 nm indicated a decrease in absorbance at a specific wavelength. As shown in Fig. 4b and c, chlorination resulted in decreased UV absorbance across wavelengths from 250 to 280 nm for each DOM fraction whether bromide ions existed or not, and bromide addition led to lower differential UV absorbance values. These observations suggested that UV-absorbing moieties in these fractions were one of the main sites where both HOCl and HOBr attacked, and appeared to be more accessible to HOCl.

The shape of the differential spectra of HPO-N shown in Fig. 4 was similar to that reported for NOM found in natural waters [30,33], showing a broad peak with a maximum at 269 and 272 nm for chlorinated samples without and with bromide addition, respectively. Korshin et al. [33] reported that the differential spectra of chlorinated NOM from several natural water sources exhibited a broad band with a maximum at a wavelength between 265 and 275 nm. Westerhoff et al. [30] also found that a band occurred at 260 nm for differential spectra of the reverse osmosis isolated NOM form Suwannee River reactions with both chlorine and bromine. However, the differential spectra of HPO-A, TPI-A and TPI-N exhibited no obvious maxima, whether bromide ions were involved in chlorination or not. The differential spectra reflected changes of the properties of chromophores in these DOM fractions during chlorination. For HPO-N, both differential spectra showed a well-defined maximum near 270 nm, suggesting that both HOCl and HOBr attacked predominantly 270 nm absorbing moieties which eventually converted into the principal reaction sites. On the contrary, the fact that there were no significant maxima in the differential spectra of HPO-A, TPI-A and TPI-N indicated the absence of predominant reaction moieties during chlorination, whose absorption occurred at a specific wavelength in the range of 250–280 nm.

3.4.2. FT-IR spectroscopic analysis

IR spectroscopy has been widely used for gross characterization of DOM and can provide valuable information on the structural and functional properties of DOM molecules [6]. The functional groups corresponding to the respective wavenumbers are shown in Table 1.

FT-IR results (Fig. 5) revealed that HPO-A, HPO-N, TPI-A and TPI-N prior to chlorination were characterized by aliphatic C–H (2950–2850 cm^{-1}, 1450 cm^{-1} and 1380 cm^{-1}), aromatic C=C (1620–1590 cm^{-1}) and aromatic C–H (875–830 cm^{-1}) peaks. The aromatic C=C peak was more prominent in HPO-A than in the others, which exhibited the highest adsorption intensity in the FT-IR spectrum of HPO-A. On the contrary, it was the peak at 1450 cm^{-1} that displayed the highest adsorption intensity in the FT-IR spectra of HPO-N, TPI-A and TPI-N. These results suggested that HPO-A had greater aromatic C=C content while HPO-N, TPO-A and TPI-N had greater aliphatic C–H content, consistent with our previous observations that HPO-A was

Table 1
General assignments of the FT-IR spectra of DOM [5,34–37]

Wavenumber (cm^{-1})	Assignment
3670–3300	OH groups
2950–2850	Aliphatic C–H, C–H_2, C–H_3 stretching
1730–1710	C=O stretching of carboxylic acids, aldehydes and ketones
1670–1650	C=O stretching of amide groups (amide I band)
1620–1590	Aromatic C=C vibration
1570–1550	N–H bending vibration of amide groups (amide II band)
1465–1440	Aliphatic C–H deformation
1420–1400	O–H bending vibration of carboxylic groups, C–O stretching of alcohols
1380–1370	C–H deformation of C–H_3 groups
1300–1000	C–O stretching of esters, ethers, phenols and alcohols
910–730	C–H bending vibration of aromatic rings
800–600	C–Cl stretching of aliphatic chloro-compounds
600–500	C–Br stretching of aliphatic bromo-compounds

among the most abundant in aromatic structures as revealed by UV analysis. Moreover, all four fractions showed weak peaks for C–O (1300–1000 cm^{-1}). Of particular interest were the significant peaks of amide-1 (1657 cm^{-1}) and amide-2 (1560 cm^{-1}) in the TPI-N spectrum, indicating amides such as peptides and *N*-acetyl amino sugars. Although HPO-N also contained amide-1 and amide-2 peaks, the amide-2 peak appeared as a minor peak and the amide-2 peak was more like a shoulder in the FT-IR spectrum. Additionally, the small peak around 1420 cm^{-1} due to carboxylic groups or alcohols was visible in the HPO-A spectrum but not in the spectra of the others.

FT-IR analysis (Fig. 5) showed that the four post-chlorination samples, which were without bromide addition, contained significant aliphatic C–H, C=O, C–O and C–Cl peaks. It was evident that aromatic structures in the four fractions were attacked by chlorine, as demonstrated by the disappearance of aromatic C–H peaks at 875–830 cm^{-1}. The results were emphasized by the significantly decreased absorption intensity of aromatic C=C peak in the TPI-A and TPI-N spectra. In addition, amides present in HPO-N and TPI-N were also attacked by chlorine as the amide peaks disappeared in the spectra of the chlorinated HPO-N and TPI-N. On the contrary, the relative absorption intensity of the C–O peak increased and the peaks for C=O and C–Cl appeared in the spectra of the four post-chlorination samples. These functional groups might have occurred as by-products from the chlorination reaction. The observations agreed with the findings of Kim and Yu [4]. They [4] reported that chlorine cleaved aromatic rings in organic molecule, producing oxygenated by-products such as carboxylic groups.

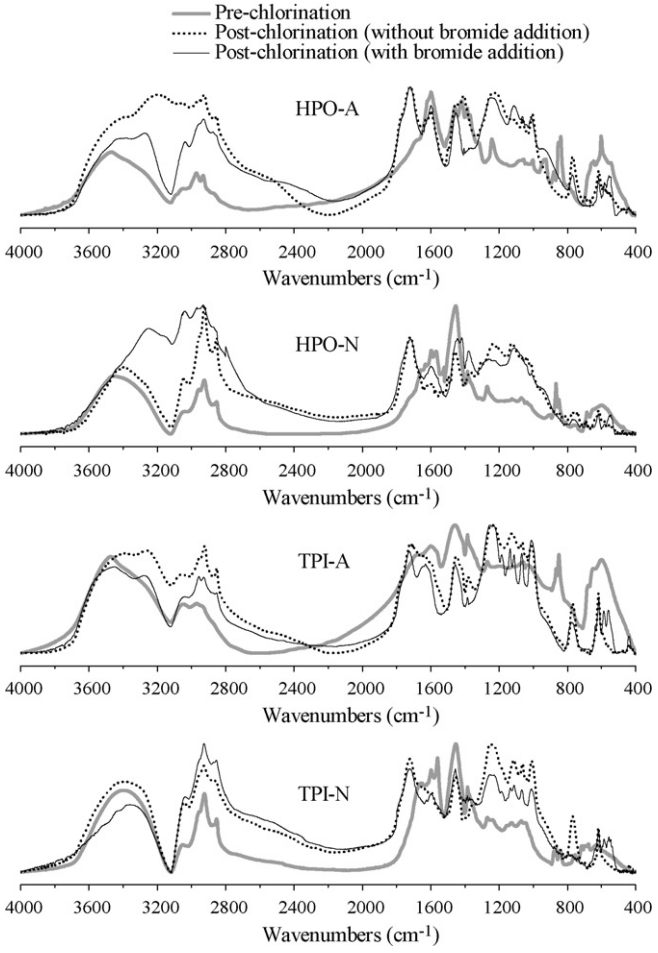

Fig. 5. FT-IR spectra of pre-chlorination DOM fractions, post-chlorination DOM fractions without bromide addition, and post-chlorination DOM fractions with bromide addition to achieve a Br^-/DOC ratio of 200 μmol/mmol.

Similarly, each post-chlorination sample with bromide addition had more intense C–O absorption intensity than the corresponding pre-chlorination sample and also contained C=O and C–Cl peaks (Fig. 5). In addition, the aromatic C–H, amide-1 and amide-2 peaks were not present in the spectra of post-chlorination samples with bromide addition. These observations suggested that HOBr and HOCl reacted with DOM in similar ways, consuming aromatic structures as well as amides and producing carboxylic acids, esters, ethers, alcohols and aliphatic chloro-compounds.

Although the spectrum of each post-chlorination sample with bromide addition showed similarities to that of the corresponding sample without bromide addition, differences in resolution and strength of some specific absorption bands were observed between the two spectra of each fraction. The most striking difference was the presence of significant C–Br peaks in the spectra of the post-chlorination samples with bromide addition, which were not visible in those without bromide addition. And the absorption intensity of C–Br peaks was quite comparable to that of C–Cl peaks in the spectra of the four post-chlorination samples, with an initial Cl_2/Br^- molar ratio of 4.2 in chlorination, suggesting that HOBr was more efficient at substituting into organic structures than HOCl. Moreover, an obvious aromatic C=C peak was present in the spectra of post-chlorination TPI-A and TPI-N with bromide addition, while it looked more like a shoulder peak in those without bromide addition. These findings implied chlorination in the absence of bromide, appeared to affect aromatic C=C in TPI-A and TPI-N, to a greater extent than chlorination with bromide addition. A weak peak around 1420 cm^{-1}, visible in the spectra of post-chlorination HPO-A without bromide addition, was not present in that with bromide addition. The functional groups corresponding to the peak around 1420 cm^{-1} in HPO-A appeared to be attacked by HOBr rather than HOCl.

4. Conclusions

The goal of this study was to investigate the effect of bromide ion on the THM formation and structure of DOM fractions during chlorination, which were isolated from the WWTP secondary effluent. The following conclusions were obtained from the study:

1. The total THM concentrations for HPO-N, TPI-A, TPI-N and HPI were fairly constant over the range of bromide concentrations studied, while HPO-A showed an increase in total THM concentration with increasing bromide concentration. The total THM concentrations for HPO-A were consistently higher than those of the other fractions. Although the total

THM concentrations varied among these fractions, the patterns of the molar concentration of individual THM species with increased bromide concentrations were similar for all fractions. The THM speciation as well as halogen fraction for these five fractions followed similar trends with the Br^-/Cl_2 ratio.

2. Based upon UV–vis spectroscopy, chlorination resulted in decreased UV absorbance across wavelengths from 250 to 280 nm for DOM fractions whether bromides ion existed or not, and bromide addition led to lower differential UV absorbance values. The HPO-N differential spectra showed a broad band with a maximum near 270 nm, whereas there were no significant maxima in the differential spectra of HPO-A, TPI-A and TPI-N, whether bromide ions were involved in chlorination or not.
3. FT-IR results indicated that chlorination, whether bromide ions existed or not, resulted in the near elimination of aromatic C–H and amide peaks, increased C–O absorption intensity and occurrence of C=O and C–Cl peaks for HPO-A, HPO-N, TPI-A and TPI-N. Furthermore, bromide addition in chlorination led to the occurrence of C–Br peak for all four fractions. Chlorination in the absence of bromide appeared to affect the absorption intensity of aromatic C=C peak for TPI-A and TPI-N to a greater extent than chlorination with bromide addition.

Acknowledgements

The authors gratefully acknowledge funding from the National Basic Research Program of China (no. 2004CB418505) and support by Program for Changjiang Scholars and Innovative Research Team in University (PCSIRT), The Ministry of Education, China.

References

[1] X. Yang, C. Shang, J.C. Huang, DBP formation in breakpoint chlorination of wastewater, Water Res. 39 (19) (2005) 4755–4767.
[2] B. Panyapinyopol, T.F. Marhaba, V. Kanokkantapong, P. Pavasant, Characterization of precursors to trihalomethanes formation in Bangkok source water, J. Hazard. Mater. 120 (1–3) (2005) 229–236.
[3] V. Kanokkantapong, T.F. Marhaba, P. Pavasant, B. Panyapinyopol, Characterization of haloacetic acid precursors in source water, J. Environ. Manage. 80 (3) (2006) 214–221.
[4] H.C. Kim, M.J. Yu, Characterization of natural organic matter in conventional water treatment processes for selection of treatment process focused on DBPs control, Water Res. 39 (19) (2005) 4779–4789.
[5] W.M. Davis, C.L. Erickson, C.T. Johnston, J.J. Delfino, J.E. Porter, Quantitative fourier transform infrared spectroscopic investigation of humic substance functional group composition, Chemosphere 38 (12) (1999) 2913–2928.
[6] J. Chen, B. Gu, E.J. LeBoeuf, H. Pan, S. Dai, Spectroscopic characterization of the structural and functional properties of natural organic matter fractions, Chemosphere 48 (1) (2002) 59–68.
[7] P.A. Maurice, M.J. Pullin, S.E. Cabaniss, Q. Zhou, K. Namjesnik-Dejanovic, G.R. Aiken, A comparison of surface water natural organic matter in raw filtered water samples, XAD, and reverse osmosis isolates, Water Res. 36 (9) (2002) 2357–2371.
[8] L. Li, Z. Zhao, W. Huang, P. Peng, G. Sheng, J. Fu, Characterization of humic acids fractionated by ultrafiltration, Org. Geochem. 35 (9) (2004) 1025–1037.
[9] G.L. Amy, P.A. Chadik, P.H. King, W.J. Cooper, Chlorine utilization during trihalomethane formation in the presence of ammonia and bromide, Environ. Sci. Technol. 18 (10) (1984) 781–786.
[10] C.Y. Chang, Y.H. Hsieh, Y.M. Lin, P.Y. Hu, C.C. Liu, K.H. Wang, The organic precursors affecting the formation of disinfection by-products with chlorine dioxide, Chemosphere 44 (5) (2001) 1153–1158.
[11] C.J. Nokes, E. Fenton, C.J. Randall, Modelling the formation of brominated trihalomethanes in chlorinated drinking waters, Water Res. 33 (17) (1999) 3557–3568.
[12] A.O. Wistrom, T. Chou, D.P.Y. Chang, E.D. Schroeder, A method for measuring haloform formation during wastewater chlorination, Water Res. 30 (12) (1996) 3146–3151.
[13] E. Koukouraki, E. Diamadopoulos, Modelling the formation of THM (trihalomethanes) during chlorination of treated municipal wastewater, Water Sci. Technol. Water Supply 3 (4) (2003) 277–284.
[14] V. Matamoros, R. Mujeriego, J.M. Bayona, Trihalomethane occurrence in chlorinated reclaimed water at full-scale wastewater treatment plants in NE Spain, Water Res. 41 (15) (2007) 3337–3344.
[15] H. Ma, H.E. Allen, Y. Yin, Characterization of isolated fractions of dissolved organic matter from natural waters and a wastewater effluent, Water Res. 35 (4) (2001) 985–996.
[16] APHA, Standard Methods for the Examination of Water and Wastewater, 20th ed., Am. Pub. Health Assoc., Washington, DC, 1998.
[17] T. Karanfil, I. Erdogan, M.A. Schlautman, Selecting filter membranes for measuring DOC and UV254, J. Am. Water Works Ass. 95 (3) (2003) 86–100.
[18] G.L. Aiken, D.M. McKnight, K.A. Thorn, E.M. Thurman, Isolation of hydrophilic organic acids from water using nonionic macroporous resins, Org. Geochem. 18 (4) (1992) 567–573.
[19] A.T. Chow, F. Guo, S. Gao, R. Breuer, Size and XAD fractionations of trihalomethane precursors from soils, Chemosphere 62 (10) (2006) 1636–1646.
[20] S. Xue, Q.L. Zhao, L.L. Wei, T. Jia, Trihalomethane formation potential of organic fractions in secondary effluent, J. Environ. Sci. -Chin. 20 (5) (2008).
[21] J.A. Leenheer, C.E. Rostad, L.B. Barber, Nature and chlorine reactivity of organic constituents from reclaimed water in groundwater, Los Angeles County, California, Environ. Sci. Technol. 35 (19) (2001) 3869–3876.
[22] W. Chen, P. Westerhoff, J.A. Leenheer, K. Booksh, Fluorescence excitation-emission matrix regional integration to quantify spectra for dissolved organic matter, Environ. Sci. Technol. 37 (24) (2003) 5701–5710.
[23] D.M. Quanrud, M.M. Karpiscak, K.E. Lansey, R.G. Arnold, Transformation of effluent organic matter during subsurface wetland treatment in the Sonoran Desert, Chemosphere 54 (6) (2004) 777–788.
[24] E.E. Chang, Y.P. Lin, P.C. Chiang, Effects of bromide on the formation of THMs and HAAs, Chemosphere 43 (8) (2001) 1029–1034.
[25] V. Uyak, I. Toroz, Investigation of bromide ion effects on disinfection by-products formation and speciation in an Istanbul water supply, J. Hazard. Mater. 149 (2) (2007) 445–451.
[26] S. Chellam, S.W. Krasner, Disinfection byproduct relationships and speciation in chlorinated nanofiltered waters, Environ. Sci. Technol. 35 (19) (2001) 3988–3999.
[27] A. Obolensky, P.C. Singer, Halogen substitution patterns among disinfection byproducts in the information collection rule database, Environ. Sci. Technol. 39 (8) (2005) 2719–2730.
[28] G. Hua, D.A. Reckhow, J. Kim, Effect of bromide and iodide ions on the formation and speciation of disinfection byproducts during chlorination, Environ. Sci. Technol. 40 (9) (2006) 3050–3056.
[29] Y. Chin, G. Aiken, E. O'Loughlin, Molecular weight, polydispersity, and spectoscopic properties of aquatic humic substances, Environ. Sci. Technol. 28 (11) (1994) 1853–1858.
[30] P. Westerhoff, P. Chao, H. Mash, Reactivity of natural organic matter with aqueous chlorine and bromine, Water Res. 38 (6) (2004) 1502–1513.
[31] C.W. Li, M.M. Benjamin, G.V. Korsin, Use of UV spectroscopy to characterize the reaction between NOM and free chlorine, Environ. Sci. Technol. 34 (12) (2000) 2570–2575.

[32] N. Ates, M. Kitis, U. Yetis, Formation of chlorination by-products in waters with low SUVA—correlations with SUVA and differential UV spectroscopy, Water Res. 41 (18) (2007) 4139–4148.
[33] G.V. Korshin, M.M. Benjamin, H.S. Chang, H. Gallard, Examination of NOM chlorination reactions by conventional and stop-flow differential absorbance spectroscopy, Environ. Sci. Technol. 41 (8) (2007) 2776–2781.
[34] L.B. Barber, J.A. Leenheer, T.I. Noyes, E.A. Stiles, Nature and transformation of dissolved organic matter in treatment wetlands, Environ. Sci. Technol. 35 (24) (2001) 4805–4816.
[35] C.F. Lin, S.H. Liu, O.J. Hao, Effect of functional groups of humic substances on UF performance, Water Res. 35 (10) (2001) 2395–2402.
[36] T.F. Marhaba, A. Mangmeechai, C. Chaiwatpongsakorn, P. Pavasant, Trihalomethanes formation potential of shrimp farm effluents, J. Hazard. Mater. 136 (2) (2006) 151–163.
[37] V. Kanokkantapong, T.F. Marhaba, B. Panyapinyophol, P. Pavasant, FTIR evaluation of functional groups involved in the formation of haloacetic acids during the chlorination of raw water, J. Hazard. Mater. 136 (2) (2006) 188–196.